

# Effect of engine oil additives reduction on the tribofilm structure of a cylinder liner model surface

*Maria de Lourdes Miranda-Medina and Christian Tomastik*

AC2T Research GmbH, Wiener Neustadt, Austria

*Tia Truglas and Heiko Groiss*

Christian Doppler Laboratory for Nanoscale Phase Transformations, Center of Surface and Nanoanalytics,  
Johannes Kepler University Linz, Linz, Austria, and

*Martin Jech*

AC2T Research GmbH, Wiener Neustadt, Austria

## Abstract

**Purpose** – The purpose of this paper is to provide a general picture for describing the formed tribofilm, including chemical and physical aspects in the micro-scale and the nano-scale. In a previous study, the durability of zinc dialkyl dithiophosphate (ZDDP) tribofilms on cylinder liner samples has been investigated in a tribometer model system by using fresh and aged fully formulated oils and replacing them with PAO8 without additives. Analyses of the derived tribofilms by means of X-ray photoelectron spectroscopy and scanning electron microscopy could give some hints about the underlying mechanisms of the tribofilm build-up and wear performance, but a final model has not been achieved.

**Design/methodology/approach** – Thus, characterisation of these tribofilms by means of focused ion beam-transmission electron microscopy (FIB-TEM) and energy dispersive X-ray spectroscopy is presented and a concluding model of the underlying mechanisms of tribofilm build-up is discussed in this paper.

**Findings** – For tribotests running first with fresh fully formulated engine oil, a rather homogeneous ZDDP-like tribofilm is found underneath a carbon rich tribofilm after changing to non-additivated PAO8. However, when the tests run first with aged fully formulated engine oil, no ZDDP-like tribofilm has been found after changing to non-additivated PAO8, but a wear protective carbon rich tribofilm.

**Originality/value** – The obtained results provide insights into the structure and durability of tribofilms. Carbon-based tribofilms are built up on the basis of non-additivated PAO8 because of the previously present ZDDP tribofilms, which suggests an alternative way to reducing the consumption of antiwear additives.

**Keywords** Wear, Tribofilm, Piston ring–cylinder liner, Zinc dialkyl dithiophosphates (ZDDPs), Transmission electron microscope (TEM), Additive depletion

**Paper type** Research paper

## 1. Introduction

Profound understanding of the impact of additives of lubricants, especially of engine oils, on the wear performance of a tribosystem requires fundamental knowledge about the morphology and composition of the related tribofilms. Among the most used and studied engine oil additives are zinc dialkyl dithiophosphates (ZDDPs). The formation mechanism and efficiency of protective layers based on ZDDP make them ideal for controlling friction and wear of steel surfaces (Spikes, 2004; Martin, 1999; Taylor *et al.*, 2008). However, ZDDP can release P, S and Zn into the environment and a frequent replacement of additivated oil is needed to retain the power and performance of the engine (Kim *et al.*, 2010). Metal-free or low

---

© Maria de Lourdes Miranda-Medina, Christian Tomastik, Tia Truglas, Heiko Groiss and Martin Jech. Published by Emerald Publishing Limited. This article is published under the Creative Commons Attribution (CC BY 4.0) licence. Anyone may reproduce, distribute, translate and create derivative works of this article (for both commercial and non-commercial purposes), subject to full attribution to the original publication and authors. The full terms of this licence may be seen at <http://creativecommons.org/licenses/by/4.0/legalcode>

The work of M. Miranda-Medina, C. Tomastik and M. Jech was funded by the Austrian COMET Programme (Project K2 XTribology, Grant No. 849109) and has been carried out within the “Austrian Excellence Center for Tribology” (AC2T research GmbH). We additional thank to the network ENTICE for providing us the samples, as well as to Prof. Anne Neville and Prof. Ardian Morina for the input ideas to develop this work. The financial support of T. Truglas and H. Groiss by the Austrian Federal Ministry for Digital and Economic Affairs and the National Foundation for Research, Technology and Development in the frame of the CDL n-phase is gratefully acknowledged. Finally, we thank to Peter Oberhumer and Sara Spiller for their collaboration during the samples preparation and acquisition of measurements.

Received 25 May 2019

Revised 14 June 2019

Accepted 14 June 2019

---

The current issue and full text archive of this journal is available on Emerald Insight at: <https://www.emerald.com/insight/0036-8792.htm>



Industrial Lubrication and Tribology  
72/4 (2020) 515–523  
Emerald Publishing Limited [ISSN 0036-8792]  
[DOI 10.1108/ILT-05-2019-0193]

content of ZDDP additives in lubricants, as well as a mixture of solutions based on ZDDP, have been investigated regarding their action to form protective films (Devlin *et al.*, 2008; Spikes, 2008; Rastogi, *et al.*, 2013). Neville and Morina studied the friction coefficient behaviour by replacing base oil (PAO6), ZDDP and molybdenum dialkyldithiocarbamate with a combination of these lubricants along a tribotest (Morina and Neville, 2007). They described the mechanism of ZDDP to maintain a low friction coefficient when it is combined with other compounds.

Investigations preferentially done by means of model or component tribotests have also shown that the ageing of the lubricants has a significant impact on the performance of the investigated system. The ageing stability depends on the chemical composition (type of additives) and stabilising agents, and the metal surfaces could act as a catalyst in the oxidation process of lubricants (Cen *et al.*, 2018). To investigate the durability of the tribofilms, Spiller *et al.* replaced additivated lubricants, in fresh and aged conditions, by non-additivated base oil PAO8 during a tribotest performed at sliding conditions. The change in dynamic wear and friction regarding the chemical composition of the antiwear films was an indicator of their durability (Spiller *et al.*, 2017). Parsaeian *et al.* investigated the impact of temperature and pressure on the growth of ZDDP tribofilms obtained from replacing fresh additivated lubricant by base oil PAO in a sliding/rolling system. The durability of these films, measured in terms of the thickness of the film, showed longer lifetime for tribofilms formed at low temperatures and pressures (Parsaeiana *et al.*, 2017).

Alternatively, the thickness and structure of the tribofilms have been investigated by transmission electron microscopy (TEM) to provide insights into the wear performance of additives (Kim *et al.*, 2010; Yu *et al.*, 2013). High-resolution TEM images have furthermore been used as reference for molecular dynamics models that simulate the digestion of abrasive particles into the zinc polyphosphate glass derived from ZDDP lubricants (Martin *et al.*, 2012). Complementarily, energy-dispersive X-ray spectroscopy (EDX) has been useful for identifying the chemical distribution of elements along a cross-section of the tribofilm (Ito *et al.*, 2006). It allows to observe the evolution of the tribofilms and formation of new/additional layers when additivated lubricants are replaced by base oil and vice versa.

In this paper, the influence of replacing additivated oils by base oils is investigated by analysing the structure of the tribofilms regarding crystallinity, elemental composition, layer structure and thickness. Our attention is focused on the tribofilms formed under sliding conditions and at 120°C, as this temperature closely corresponds to the application regime in an engine.

## 2. Experimental methods and sample description

### 2.1 Samples and specific knowledge base

In a previous study carried out by Spiller *et al.* (2017), the tribofilm build-up with respect to additive availability has been investigated for the tribosystem piston ring against cylinder liner in a tribometer set-up (Lenauer *et al.*, 2014). The piston ring is made of nitrided X90CrMoV18 steel, the cylinder liner is composed of grey cast iron with lamellar graphite and a

chemical composition of 4 per cent C, 0.8 per cent P, 1.1 per cent Cr, 1.4 per cent Mn and 2.4 per cent Si (with Fe the balance). The tribometer tests were carried out with an SRV® and a load of 200 N, a frequency of 6 Hz, a stroke of 3 mm and an oil temperature of 120°C. Tests were also carried out at 20°C, but in the present paper, the focus was on the samples run at 120°C because of a closer link to engine applications.

The tribotests were carried out by the following procedure: for the first period of 7 h (Period 1), the tribotests were run with fully formulated engine oil, then the oil circuit was cleaned and flushed and subsequently run in the second period for 25 h with non-additivated PAO8 (Period 2). The fully formulated engine oil has been applied at two conditions: fresh as purchased and altered in laboratory equipment. The following abbreviations are used in this paper for characterising the lubricant and for the tribotest conditions with the mentioned lubricants:

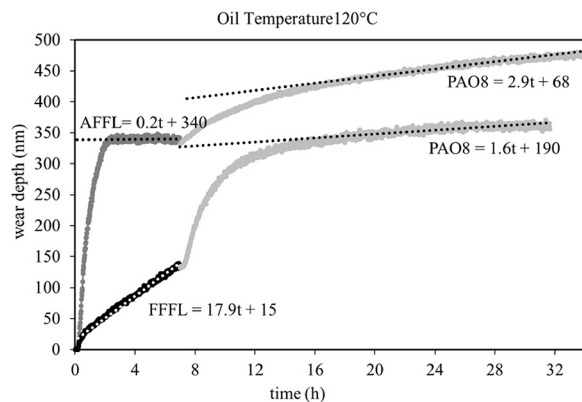
- FFFL – fresh fully formulated lubricant;
- AFFL – aged fully formulated lubricant;
- FFFL + PAO8 – first run with FFFL and then run with PAO8; and
- AFFL + PAO8 – first run with AFFL and then run with PAO8.

The durability of the tribofilms was investigated in Spiller *et al.* (2017) by comparing the dynamic wear behaviour, determined by radio isotope concentration method (Jech and Lenauer, 2017), friction behaviour and the chemical composition of the worn surfaces, determined by X-ray photoelectron spectroscopy (XPS).

The findings from Spiller *et al.* (2017) are summarised in the following, with regard to the further discussion with the results of the present paper:

- 1 There is a clear difference in the wear performance, when comparing the fresh and aged conditions (Figure 1).
  - There is hardly any running-in and a relatively high steady-state wear rate in the first 7 h (Period 1) with the FFFL when compared with the AFFL.

**Figure 1** Recapitulation of wear curves (Spiller *et al.*, 2017): tests run first for 7 h (Period 1) in fresh (black) or aged (dark grey) fully formulated engine oil, and subsequently for 25 h (Period 2) in non-additivated PAO8 oil (light grey) at 120°C



**Notes:** The dotted lines represent the fitting for deriving the running-in and steady-state wear values. Numerical data are given in (nm). The wear curves are an average presentation of two independent tests each

- When changing to PAO8 after 7 h (Period 2), the FFFL + PAO8 shows a remarkably high running-in when compared with the AFFL + PAO8.
  - Both conditions finally lead to a similar total-wear height and low and stable steady-state wear rate in the range of a few nano-meters per hour.
- 2 An increasing wear trend (divergent wear) has not been observed after changing to non-additivated oil, as could have been expected. This has been explained by the presence of a robust ZDDP tribofilm and consequently by the time (in terms of stable wear conditions) given for building up a carbon-rich tribofilm during additive-depleted conditions. It seems that phosphor (e.g. phosphate) has been exchanged (partially) by carbon (Figure 2).
  - 3 The comparison of chemical composition of the different tribofilms (Figure 2) shows that the amount of carbon increases with additive depletion, whereas the amount of additive elements, such as Ca (detergent), P, S and Zn (elements of ZDDP), decreases. The elemental composition shown in Figure 2 was obtained by XPS measurements of the top surface region after sputter cleaning for 30 s, which corresponds to a sputtered depth approximately of 6 nm.

This paper aims at a further clarification of the structure and build-up of the tribofilms described in Spiller *et al.* (2017) by characterisation of the profile and texture of the tribofilm perpendicular to the surface. This is done by cutting lamellae out of the wear scar by means of a focused ion beam (FIB) and subsequent analysis by TEM, scanning transmission electron microscopy (STEM) and EDX.

## 2.2 Sample preparation for transmission electron microscopy measurements

After the tribometer tests, the samples were briefly rinsed in petroleum ether [Figure 3(a)]. A gold layer of approximately 100 nm thickness was sputtered onto the samples to protect the tribofilm structure (Dawczyk *et al.*, 2018). The wear scar area [Figure 3(b)] was marked by carbon dots to have contrast layers for the detection of the tribofilm. Then TEM lamellae were prepared with a ZEISS 1540 XB FIB instrument. To this

**Figure 2** Representation of XPS results for top surface layer of (a) FFFL, (b) FFFL + PAO8, (c) AFFL and (d) AFFL + PAO8, referring to (Spiller *et al.*, 2017)

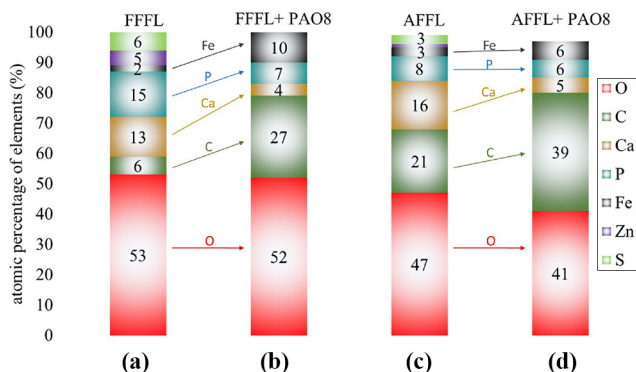
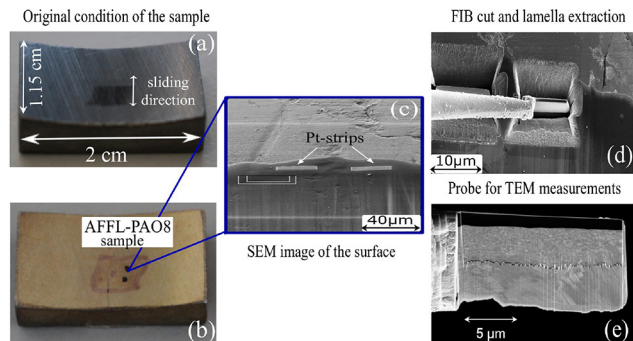


**Figure 3** Sample preparation for TEM and STEM images



**Notes:** (a) AFFL + PAO8 original sample after the tribotest; (b) contrast layers: sputtered gold layer (100 nm) and carbon marks on the selected area; (c) deposition of Pt protective strips; (d) Lamella lift-out at FIB cut; (e) thinned TEM lamella

end, a protective Pt layer was deposited on top of the gold layer [Figure 3(c)], followed by the cut-out of the TEM lamella [Figure 3(d)]. After the lift-out [Figure 5(e)], the lamella was finally thinned to electron transparency for TEM investigations, with a length between 10 and 15  $\mu\text{m}$ , a height of 10  $\mu\text{m}$  and a thickness of approximately 170 nm.

The lamellae were analysed with a Jeol JEM-2200FS TEM, which is equipped with a field emitter gun and was operated at 200 kV for these measurements. For chemical/elemental analysis, an attached Oxford EDX System was used. Conventional TEM images and diffraction patterns were acquired with a 4k  $\times$  4k TVIPS CMOS camera. For STEM imaging, a bright field and a high-angle annular dark field detector were used.

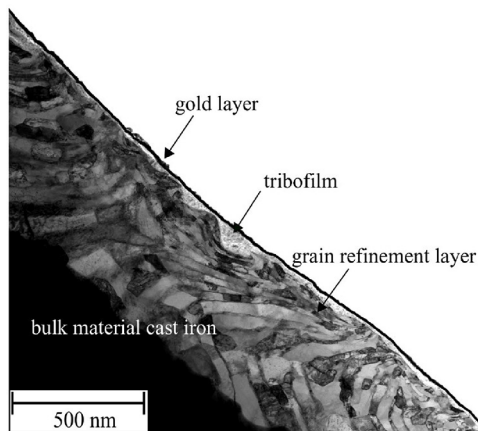
As a TEM lamella contains only a small volume of the sample, the lift-out positions were chosen in the SEM to be as representative as possible for the macroscopic wear scar. To increase the significance of the TEM results, six analyses at different positions at two lamellae were made for AFFL + PAO8 and five analyses at different positions at one lamella for FFFL + PAO8. In the following, representative and typical pictures of the structure of the corresponding tribofilms are given.

## 3. Results

### 3.1 Structure of the tribofilms by transmission electron microscopy images

The high resolution achievable with TEM measurements allows for differentiation of grains, as well as composition, and is therefore especially suitable for investigating the tribofilm layer derived from sliding processes. Figure 4 shows the deformation and refinement of grains from the bulk material near to the surface for the samples obtained from AFFL + PAO8. The grain refinement close to the contact surface is a well-known effect and depends on the material, as well as the tribological loading conditions (Olander *et al.*, 2013; Sanabria *et al.*, 2014). In the present study, the impact of the initial condition of the lubricant is investigated regarding the formation of a tribofilm on top of the grain refinement layer. The deposited tribofilm is visible as a bright layer of changing thickness between the grain structure and the gold layer in Figure 4. Regarding the use of the term “tribofilm” in the present

**Figure 4** STEM bright field image of the tribofilm layer derived from the sliding process for aged fully formulated oil changed to PAO8 oil (AFFL + PAO8)



paper, tribofilms are understood by the authors as mainly consisting of elements from the lubricant. They may contain some layers with mixtures of elements or particles from the substrate, either directly eroded from the substrate or reinserted wear particles. Further, the tribofilm is referred to as chemisorbed tribofilm, as physisorbed elements may have been removed by the necessary processing for TEM preparation, such as rinsing or cleaning.

Close-up images of the tribofilm with different scales are presented in Figure 5. The top part of Figure 5 shows details of the tribofilm obtained from FFFL + PAO8, while the bottom part shows details of the tribofilm obtained from AFFL + PAO8.

A clear difference between the two kinds of tribofilm is observed regarding the thickness and film appearance. For FFFL + PAO8 (Figure 5, top) a thickness of 10–40 nm is observed for the tribofilm that appears rather constant in thickness with a remarkable light line going through the

tribofilm parallel to the surface. For AFFL + PAO8 (Figure 5, bottom) the film thicknesses varies from 5 to 130 nm. The AFFL + PAO8 lubricant seems to accumulate in the dimples of the worn surface. Dimples were not observed in the TEM pictures of the FFFL + PAO8 tribofilms; it has to be assumed for the AFFL + PAO8 tribofilm that the dimple-like structure and tribofilm accumulation develop simultaneously or even cause each other.

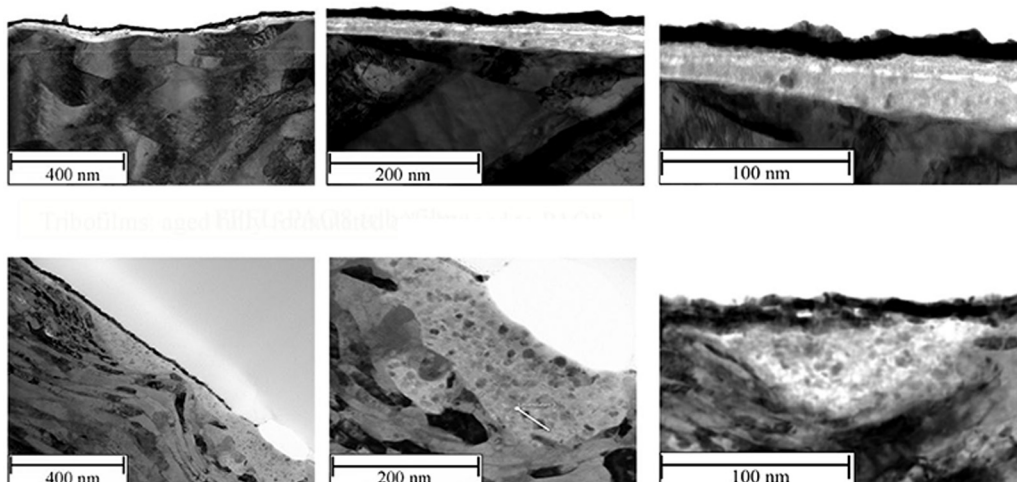
For clarity, roughness features in the present study, such as grooves, dimples or tops, are related to the substrate surface, whereas a topographic measurement of a surface would capture the topographic features of the whole sliding surface as a superposition of substrate and tribofilm.

A lower wear rate is expected for thicker tribofilms, the thickness being an indicator of the durability (Suominen Fuller et al., 2008). Based on the tribofilm thickness obtained by these TEM measurements, a prediction of the corresponding wear performance in terms of wear rate seems to be difficult, especially for the AFFL + PAO8 condition. The wear rate for both conditions is similar at the test end, both tribofilm conditions can be regarded as wear-protective and thus functional, which at first glance cannot be attributed regarding the thickness here.

### 3.2 Investigation of morphology by transmission electron microscopy diffraction mode

The morphological and structural details of the tribofilm and grain refinement region were investigated by selected area of the sample, from which a spot diffraction pattern is generated at parallel illumination. The main phase constituent in cast iron is ferrite, which has a body-centered cubic crystal structure. A single ferrite grain orientated along a certain zone axis shows a characteristic diffraction pattern with the allowed diffraction reflexes. However, when a small number of differently oriented grains lay within the selected area, the SAD pattern shows the sum of all captured orientations. The more crystallites with random orientations are present, the more the spots begin to

**Figure 5** STEM bright field images with different scales obtained from tribofilms formed under two conditions



**Notes:** Top images: FFFL + PAO8; bottom images: AFFL + PAO8

form diffraction rings as seen in Figure 6(b), (c) and (d). The ring radii represent the inter-plane distances of the respective specific crystal structures in reciprocal space. When comparing Figure 6 (b) and (c) to Figure 6 (d), a higher number of bright spots signifies a higher number of grains, which implies a smaller grain size in the tribofilm compared to the grain refinement region. Different number and distances of the diffraction rings indicate different phases in the respective regions.

Figure 6(e) and (f) show the radial summed-up diffraction profile of (b) and (c). The peak at zero corresponds to the (000) direct beam, while the consecutive peaks are the reciprocal distances between planes derived from one component. The peaks of the AFFL + PAO8 tribofilm and the grain refinement layer are compared to theoretical values obtained from the Java-based electron microscopy simulation software (Stadelmann, 2014). Thus, the corresponding compound, as well as the lattice planes (miller indices h, k and l), are determined.

Figure 6(e) shows reflexes, where at least three significant ones can be assigned to the Au protection layer. The other

closely spaced ones originate from Fe<sub>3</sub>C and iron oxide grains, e.g. Fe<sub>2</sub>O<sub>3</sub> and Fe<sub>3</sub>O<sub>4</sub>, which are embedded in the amorphous carbon matrix.

Figure 6(f) shows that the grain refinement zone (blue graph) consists of almost only ferrite grains, and all strong reflexes come from this material phase. Some minor reflexes are referred to oxides and carbides at the grain boundaries (not indicated in the graph).

In the following, crystallographic details of the tribofilm on top of the substrate are depicted.

Figure 7 highlights details of the FFFL + PAO8 tribofilm, where a layer structure is apparent, especially in the form of a light layer in the middle of the tribofilm separating an upper and a lower layer. The upper and middle layers show dominantly amorphous structures, whereas the lower layer shows partially crystalline structures embedded in an amorphous surrounding.

A different picture is obtained for the AFFL + PAO8 tribofilm. The tribofilm consists of amorphous host matrix with

Figure 6 (a) TEM image from tribofilm and surface near structure for AFFL + PAO8; circles mark the regions selected by the SAD aperture, diffraction patterns of (b) tribofilm, (c) grain refinement and (d) bulk material; interplanar distance of (e) the tribofilm (green) and (f) the grain refinement zone (blue)

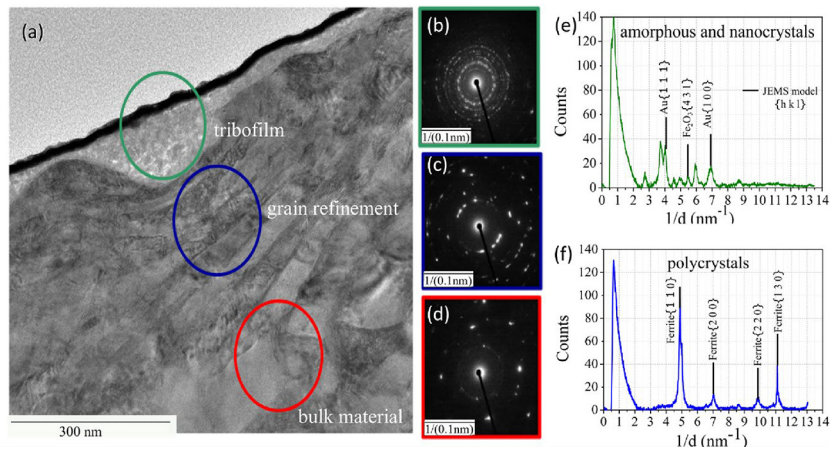
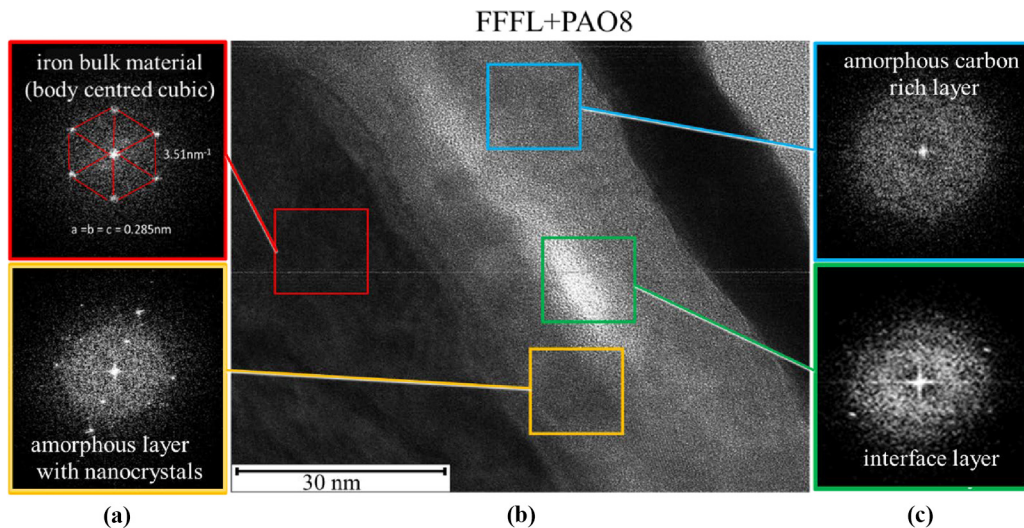


Figure 7 High-resolution TEM images, details of selected regions and Fourier transform patterns of selected regions of the FFFL + PAO8 tribofilm



embedded iron oxide nanocrystals. The iron oxide particles seem to be homogeneously distributed in the tribofilm and no additional structure is observed within the AFFL + PAO8 tribofilm (Figure 8).

### 3.3 Elemental composition of the tribofilms by X-ray spectroscopy evaluation

For further clarification of the tribofilm structure, elemental compositions of the different layers are investigated by EDX.

*EDX of FFFL + PAO8:* The upper layer of the FFFL + PAO8 tribofilm contains a high percentage of C, is approximately 10 nm thick and further denominated as carbon layer, in the sense of a carbon-rich layer. In the lower layer, which is closer to the substrate and 20–30 nm thick, P, Ca and Zn were detected [Figure 9(b) and (d)]. As P and Zn are present in ZDDP and Ca known as a detergent element, the lower layer can be regarded as the additive-rich layer and thus denoted as ZDDP layer. The EDX does not reveal the composition of the thin bright line in between the upper and lower tribofilms, which is most probably a porous transition area between the two layers.

Additionally, the EDX data obtained along the tribofilm confirm the presence of embedded iron-rich particles, as highlighted by a circle in Figures 9(a) and (c). The embedded particles, which have sizes varying between 5 and 15 nm, are found at all analysed spots (not shown here).

*EDX of AFFL + PAO8:* The results obtained from EDX measurements near to the surface of sample AFFL + PAO8 [Figure 10(c), (d)] show that the tribofilm mainly consists of O up to 60 per cent, Fe in the range of 20–30 per cent and C in the range of 10–20 per cent. It is concluded that the tribofilm investigated at this spots is mainly consisting of iron-oxide particles embedded in carbon, which is deposited from the lubricant.

## 4. Discussion

The TEM results reveal that the investigated tribofilms after Period 2 are significantly different because of conditions in

Period 1, when the tribosystem was either run with fresh or aged fully formulated engine oil (Figure 5). This means that the tribofilm structure is significantly influenced by the pre-existing tribofilm of Period 1, as well as by the depletion of additives in Period 2. Unfortunately, the samples specifically run just in Period 1 have not been available for the present TEM investigations. However, the XPS results of the samples of Period 1 (Figure 2) are in general agreement to state-of-the-art literature; therefore, we are convinced that a differentiated description is also possible with only TEMs after Period 2.

*Tribofilm of FFFL + PAO8:* At those spots of the TEM lamellae which have been analysed by EDX (Figure 9), the elements of the ZDDP additive are not significantly detected in the top layer (concentration lower than 1 per cent). This is in accordance to the XPS analysis done at the same sample (Spiller et al., 2017). However, while Fe and C concentrations are in a comparable range, the O concentration from XPS is much higher (approximately 50 At.%) than from EDX (25–30 At.%). Through XPS a thin surface layer (few nm) is analysed but averaged over a comparable large lateral area (in case of Spiller et al., 2017, with a spot diameter of 400  $\mu\text{m}$ ). The presented TEM-EDX measurements are the results of line scans over a selected region in the nm range. This impedes a direct linking of the results from these techniques. Underneath the carbon tribofilm (top layer), an additive-rich tribofilm with elements of ZDDP, such as Zn and P, as well as Ca as detergent element, has been found.

*Tribofilm of AFFL + PAO8:* In the AFFL + PAO8 tribofilm additive elements could not be found in a significant amount (lower than 1 per cent). The morphology of this tribofilm does not show any internal layer structure. The crystallographic investigation revealed a high amount of embedded iron-oxide particles in a carbon deposit. These particles are detached either from the cylinder liner or from the counterpart and reincorporated during the tribotests.

**Figure 8** High-resolution TEM images, details of selected regions and Fourier transform patterns of selected regions of the AFFL + PAO8 tribofilm

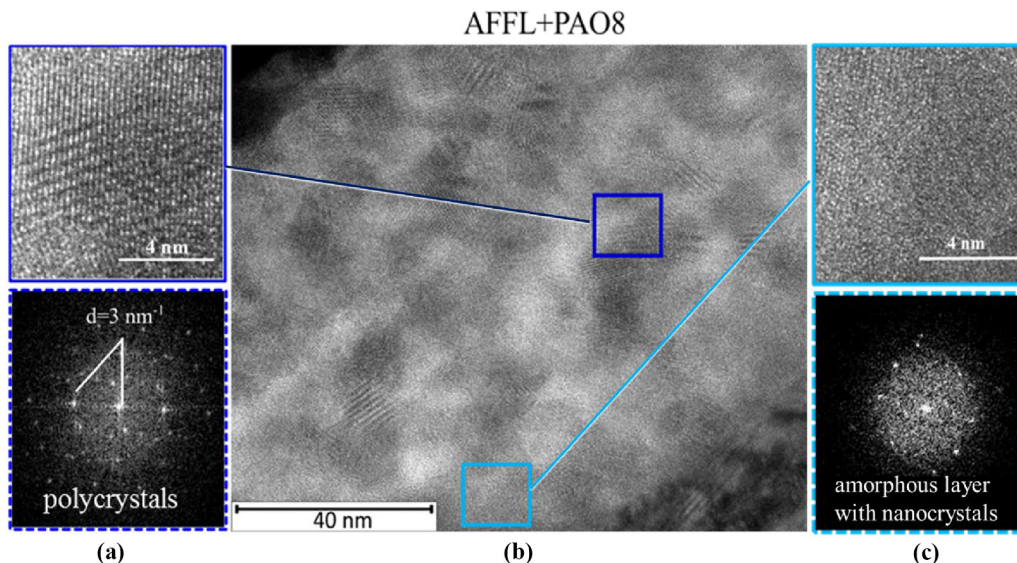


**Figure 9** (a) STEM image of FFFL + PAO8; EDX chemical composition; (b) across and (c) along the tribofilm; (d) shows a detail of (b)

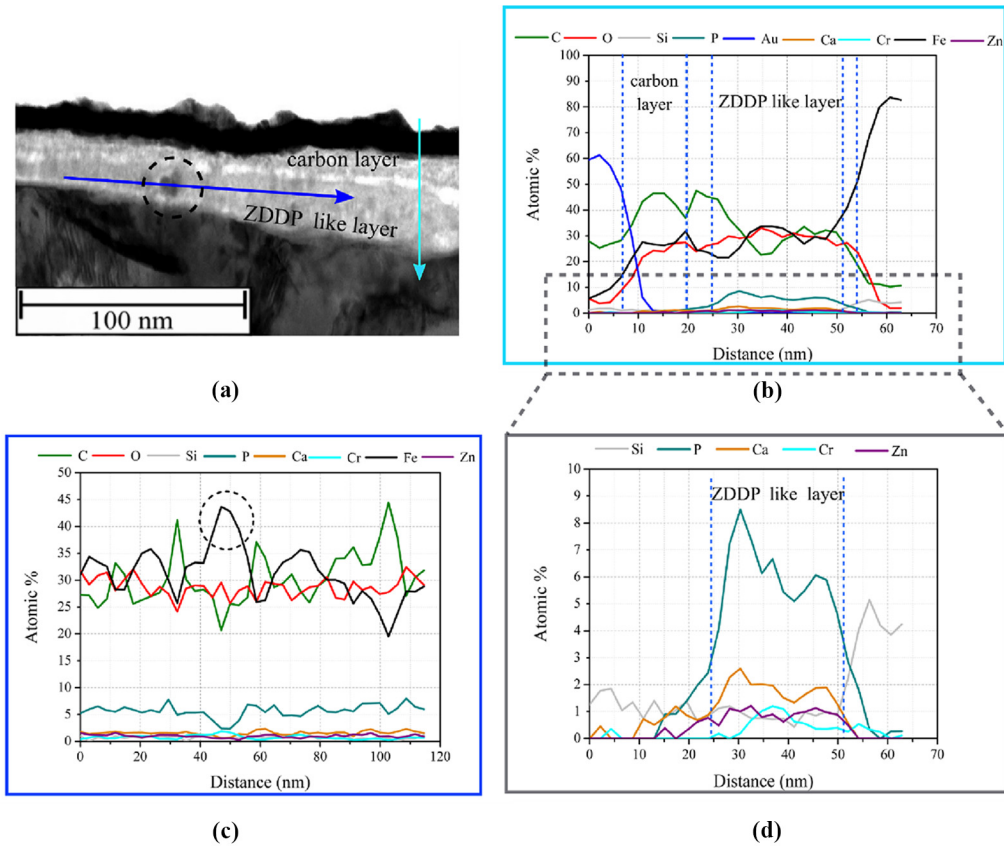
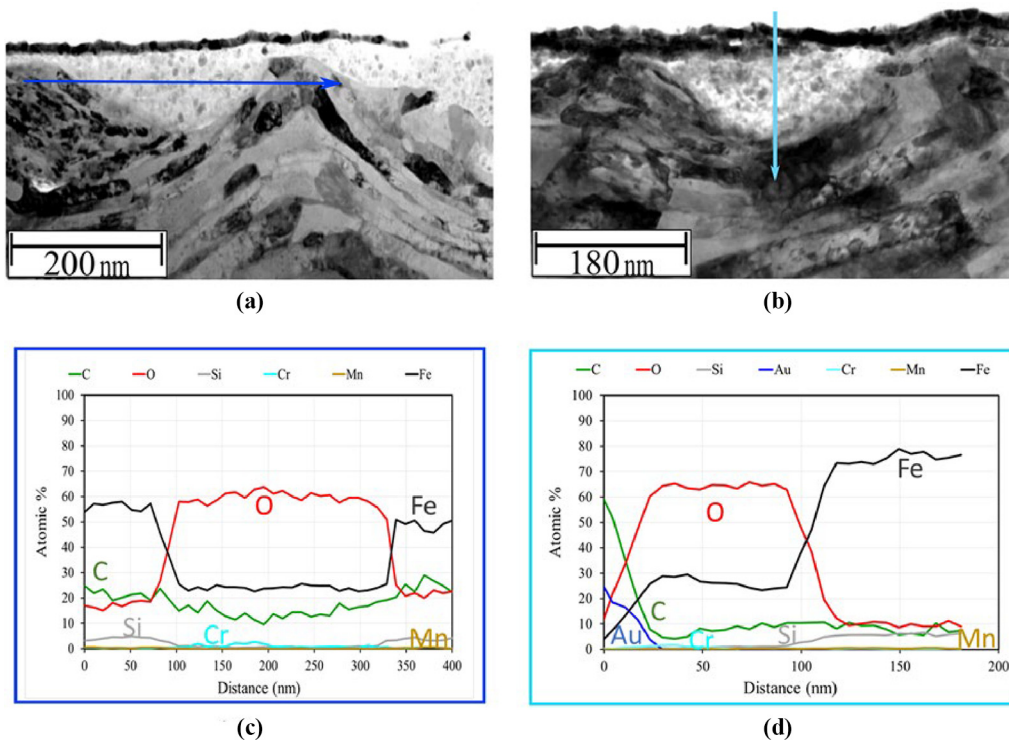


**Figure 10** (a) and (b) STEM images of tribofilm formed from aged fully formulated oil changed to PAO8 (AFFL + PAO8). EDX chemical composition (c) along the tribofilm in spot (a) and (d) across the tribofilm at spot (b)



#### 4.1 Model of tribofilm build-up

Although stable and comparable behaviours have been observed for FFFL + PAO8 and AFFL + PAO8 in terms of total wear height, steady-state wear rate (Figure 1), and chemical composition of the tribofilms (Figure 2), the variation in the running-in wear phases suggests structural differences in the formation and structure of the tribofilms (Figures 11 and 12).

Considering the interpretation of the above-presented experimental results, the authors would like to discuss models for the different tribofilm build-up:

*Tribofilm build-up of FFFL + PAO8:* The combination of three factors, namely, shear force, high temperature and additivated lubricant, leads to the formation of a ZDDP-like tribofilm on top of an oxide layer during Period 1. The running-in is rather small compared to the running-in of the aged condition; therefore, hardly any smoothing of the initial roughness is expected with the fresh condition.

**Figure 11** AFM, STEM, EDX data and corresponding schematic structure of the tribofilms derived from fresh fully formulated lubricants replaced by PAO8 (FFFL+PAO8)

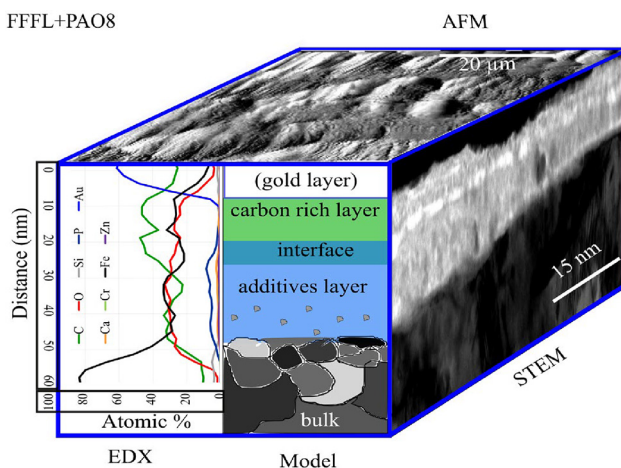
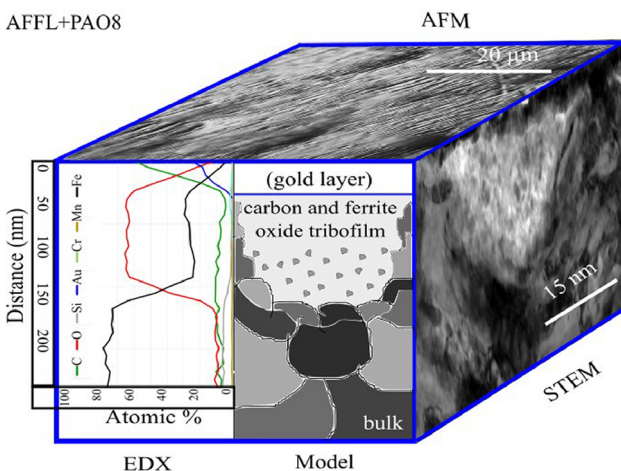


**Figure 12** AFM, STEM, EDX data and corresponding schematic structure of the tribofilms derived from aged fully formulated lubricants replaced by PAO8 (AFFL+PAO8)



The FFFL steady-state wear is remarkably high when compared to the steady-state wear rate of AFFL and considering that ZDDP-like tribofilms are regarded to be wear-protective. Regarding the wear rate of FFFL, a steady wear of the substrate accompanied by the steady removal and build-up of the ZDDP tribofilm is assumed.

When changing to PAO8 oil, a high running-in is observed at the beginning of Period 2, signifying a reduction of the ZDDP protective layer and giving rise to an amorphous carbon-based tribofilm (Figure 11). The steady-state wear rate of FFFL + PAO8 is remarkably low, especially considering that no additives are available in the lubricant. It is assumed that the carbon-rich tribofilm provides excellent wear-protective characteristics.

*Tribofilm build-up of AFFL + PAO8:* The high running-in during Period 1 at AFFL conditions suggests that because of shear and wear a groove- and dimple-like structure of the substrate surface was formed. Wear particles, such as iron oxides, together with carbon, such as lubricant components, were deposited in these dimples (Figure 12). Considering that the wear measurement based on radioactive isotopes (Jech and Lenauer, 2017) mainly detects wear from the activated substrate material, the material in the dimples does not contribute to the measured wear signal any more. Further, it is unlikely that a wear-protective ZDDP tribofilm forms on the area covered by the deposited material. Instead, it is presumed that a ZDDP-like tribofilm forms because of shearing only at the tops of the substrate surface. This is regarded as the end of the running-in, and further wear is just assumed to occur at these tops, which are only a fraction of the total sliding surface.

The steady-state wear is close to zero, which is a well-known observation with aged lubricants (Lenauer et al., 2014). The authors expect wear to occur just at (the surface/top layers of) the tribofilm and thus not reaching the substrate material. The presence of aged and thus oxidised additives provides a prompt reproduction of the worn tribofilm.

When changing to additive-depleted conditions by changing to non-additivated PAO8, the ZDDP-like tribofilms on the tops are removed, which can be observed as a new running-in. As these tops are only a fraction of the sliding surface, the running-in wear amount is comparably moderate. Owing to the pre-existence of a tribofilm, a new tribofilm forms or the existing tribofilm evolves in such a way that the carbon tribofilm provides an effective wear protection at additive-depleted conditions. In the following steady-state wear regime, wear is expected just from the tops of the substrate.

## 5. Conclusion

By subsequent TEM analysis of samples run with different oils and depletion of additives, a detailed picture of a local tribofilm structure has been obtained:

- When run with fresh fully formulated engine oil and exchanged to non-additivated PAO8 a layer structure of the tribofilm is observed, in which still a homogeneous ZDDP-like layer was present and covered by a carbon rich layer.
- When run with aged fully formulated engine oil and exchanged to non-additivated PAO8 a dimple-like surface structure is observed with unevenly distributed tribofilm,

which mainly consists of iron oxide particles with carbon deposits.

- Although there is a remarkably different structure observed for the two kinds of tribofilms, the wear performance is rather similar with wear rates. This suggests that the tribofilms are efficient in wear protection of the initial material. As such, the carbon deposit tribofilm may provide an alternative way to reduce the consumption of antiwear additives and consequently their environmental impact.

## References

- Cen, H., Morina, A. and Neville, A. (2018), "Effect of lubricant ageing on lubricant physical and chemical properties and tribological performance, Part I: effect of lubricant chemistry", *Industrial Lubrication and Tribology*, Vol. 70 No. 2.
- Dawczyk, J., Ware, E., Ardakani, M., Russo, J. and Spikes, H. (2018), "Use of FIB to study ZDDP tribofilms", *Tribology Letters*, Vol. 66 No. 4, pp. 2-8.
- Devlin, M.T., Guevremont, J., Sheets, R., Loper, J., Guinther, G., Thompson, K. and Jao, T.-C. (2008), "Effect of metal-free phosphorus anti-wear compounds on", *Lubrication Science*, Vol. 20 No. 2, pp. 151-161.
- Ito, K., Martin, J.M., Minfray, C. and Kato, K. (2006), "Low-friction tribofilm formed by the reaction of ZDDP on iron oxide", *Tribology International*, Vol. 39 No. 12, pp. 1538-1544.
- Jech, M. and Lenauer, C. (2017), "Radionuclide methods", *ASM Handbook, Volume 18: Friction, Lubrication, and Wear Technology*, ASM International, pp. 1045-1055.
- Kim, B., Mourhatch, R., B. and Aswath, P. (2010), "Properties of tribofilms formed with ashless dithiophosphate and zinc dialkyl dithiophosphate under extreme pressure conditions", *Wear*, Vol. 268 Nos 3/4, pp. 579-591.
- Lenauer, C., Tomastik, C., Wopelka, T. and Jech, M. (2014), "Piston ring wear and cylinder liner tribofilm in tribotests with lubricants artificially altered with ethanol combustion products", *Tribology International*, Vol. 82 (18 June), pp. 415-422.
- Martin, J.M. (1999), "Antiwear mechanisms of zinc dithiophosphate: a chemical hardness approach", *Tribology Letters*, Vol. 6 No. 1, pp. 1-8.
- Martin, J.M., Onodera, T., Minfray, C., Dassenoy, F. and Miyamoto, A. (2012), "The origin of anti-wear chemistry of ZDDP", *Faraday Discussions*, Vol. 156, pp. 311-323.
- Morina, A. and Neville, A. (2007), "Understanding the composition and low friction tribofilm formation/removal in boundary lubrication", *Tribology International*, Vol. 40 Nos 10/12, pp. 1696-1704.
- Olander, P., Hollman, P. and Jacobson, S. (2013), "Piston ring and cylinder liner wear aggravation caused by transition to greener ship transports-Comparison of samples from test rig and field", *Wear*, Vol. 302 Nos 1/2, pp. 1345-1350.
- Parsaeian, P., Ghanbarzadeh, A., Van Eijk, M.C.P., Nedelcu, I., Neville, A. and Morina, A. (2017), "A new insight into the interfacial mechanisms of the tribofilm formed by zinc dialkyl dithiophosphate", *Applied Surface Science*, Vol. 403, pp. 472-486.
- Rastogi, R., Maurya, J. and Jaiswal, V. (2013), "Low sulfur, phosphorus and metal free antiwear additives: synergistic action of salicylaldehyde N(4)-phenylthiosemicarbazones and its different derivatives with vanlube 289 additive", *Wear*, Vol. 297 Nos 1/2, pp. 849-859.
- Sanabria, V., Mueller, S. and Reimers, W. (2014), "Microstructure evolution of friction boundary layer during extrusion of AA 6060", *Procedia Engineering*, Vol. 81, pp. 586-591.
- Spikes, H. (2004), "The history and mechanisms of ZDDP", *Tribology Letters*, Vol. 17 No. 3, pp. 469-489.
- Spikes, H. (2008), "Low- and zero-sulphated ash, phosphorus and sulphur anti-wear additives for engine oils", *Lubrication Science*, Vol. 20 No. 2, pp. 103-136.
- Spiller, S., Lenauer, C., Wopelka, T. and Jech, M. (2017), "Real time durability of tribofilms in the piston ring - cylinder liner contact", *Tribology International*, Vol. 113, pp. 92-100.
- Stadelmann, P. (2014), "JEMS-SAAS ems java version V4", available at: [www.jems-saas.ch/Home/jemsWebSite/jems.html](http://www.jems-saas.ch/Home/jemsWebSite/jems.html) (accessed 3 September 2018).
- Suominen Fuller, M.L., Rodriguez Fernandez, L., Massoumi, G.R., Lennard, W.N., Kasrai, M. and Bancroft, G.M. (2008), "The use of X-ray absorption spectroscopy for monitoring the thickness of antiwear films from ZDDP", *Tribology Letters*, Vol. 8 No. 4, pp. 187-192.
- Taylor, L., Dratva, A. and Spikes, H.A. (2008), "Friction and wear behavior of zinc dialkyldithiophosphate additive", *Tribology Transactions*, Vol. 43 No. 3, pp. 469-479.
- Yu, H., Xu, Y., Shi, P., Wang, H., Wei, M., Zhao, K. and Xu, B. (2013), "Microstructure, mechanical properties and tribological behavior of tribofilm generated from natural serpentine mineral powders as lubricant additive", *Wear*, Vol. 297, pp. 802-810.

## Corresponding author

Maria de Lourdes Miranda-Medina can be contacted at: [maria.miranda@ac2t.at](mailto:maria.miranda@ac2t.at)